

Absolute Branching Fraction Measurements for D^+ and D^0 Inclusive Semileptonic Decays

N. E. Adam,¹ J. P. Alexander,¹ K. Berkelman,¹ D. G. Cassel,¹ J. E. Duboscq,¹ K. M. Ecklund,¹ R. Ehrlich,¹ L. Fields,¹ L. Gibbons,¹ R. Gray,¹ S. W. Gray,¹ D. L. Hartill,¹ B. K. Heltsley,¹ D. Hertz,¹ C. D. Jones,¹ J. Kandaswamy,¹ D. L. Kreinick,¹ V. E. Kuznetsov,¹ H. Mahlke-Krüger,¹ T. O. Meyer,¹ P. U. E. Onyisi,¹ J. R. Patterson,¹ D. Peterson,¹ J. Pivarski,¹ D. Riley,¹ A. Ryd,¹ A. J. Sadoff,¹ H. Schwarthoff,¹ X. Shi,¹ S. Stroiney,¹ W. M. Sun,¹ T. Wilksen,¹ M. Weinberger,¹ S. B. Athar,² R. Patel,² V. Potlia,² H. Stoeck,² J. Yelton,² P. Rubin,³ C. Cawfield,⁴ B. I. Eisenstein,⁴ I. Karliner,⁴ D. Kim,⁴ N. Lowrey,⁴ P. Naik,⁴ C. Sedlack,⁴ M. Selen,⁴ E. J. White,⁴ J. Wiss,⁴ M. R. Shepherd,⁵ D. Besson,⁶ T. K. Pedlar,⁷ D. Cronin-Hennessy,⁸ K. Y. Gao,⁸ D. T. Gong,⁸ J. Hietala,⁸ Y. Kubota,⁸ T. Klein,⁸ B. W. Lang,⁸ R. Poling,⁸ A. W. Scott,⁸ A. Smith,⁸ S. Dobbs,⁹ Z. Metreveli,⁹ K. K. Seth,⁹ A. Tomaradze,⁹ P. Zweber,⁹ J. Ernst,¹⁰ H. Severini,¹¹ S. A. Dytman,¹² W. Love,¹² V. Savinov,¹² O. Aquines,¹³ Z. Li,¹³ A. Lopez,¹³ S. Mehrabyan,¹³ H. Mendez,¹³ J. Ramirez,¹³ G. S. Huang,¹⁴ D. H. Miller,¹⁴ V. Pavlunin,¹⁴ B. Sanghi,¹⁴ I. P. J. Shipsey,¹⁴ B. Xin,¹⁴ G. S. Adams,¹⁵ M. Anderson,¹⁵ J. P. Cummings,¹⁵ I. Danko,¹⁵ J. Napolitano,¹⁵ Q. He,¹⁶ J. Insler,¹⁶ H. Muramatsu,¹⁶ C. S. Park,¹⁶ E. H. Thorndike,¹⁶ T. E. Coan,¹⁷ Y. S. Gao,¹⁷ F. Liu,¹⁷ M. Artuso,¹⁸ S. Blusk,¹⁸ J. Butt,¹⁸ J. Li,¹⁸ N. Menea,¹⁸ R. Mountain,¹⁸ S. Nisar,¹⁸ K. Randrianarivony,¹⁸ R. Redjimi,¹⁸ R. Sia,¹⁸ T. Skwarnicki,¹⁸ S. Stone,¹⁸ J. C. Wang,¹⁸ K. Zhang,¹⁸ S. E. Csorna,¹⁹ G. Bonvicini,²⁰ D. Cinabro,²⁰ M. Dubrovin,²⁰ A. Lincoln,²⁰ D. M. Asner,²¹ K. W. Edwards,²¹ R. A. Briere,²² I. Brock,^{22,*} J. Chen,²² T. Ferguson,²² G. Tatishvili,²² H. Vogel,²² M. E. Watkins,²² and J. L. Rosner²³

(CLEO Collaboration)

¹Cornell University, Ithaca, New York 14853

²University of Florida, Gainesville, Florida 32611

³George Mason University, Fairfax, Virginia 22030

⁴University of Illinois, Urbana-Champaign, Illinois 61801

⁵Indiana University, Bloomington, Indiana 47405

⁶University of Kansas, Lawrence, Kansas 66045

⁷Luther College, Decorah, Iowa 52101

⁸University of Minnesota, Minneapolis, Minnesota 55455

⁹Northwestern University, Evanston, Illinois 60208

¹⁰State University of New York at Albany, Albany, New York 12222

¹¹University of Oklahoma, Norman, Oklahoma 73019

¹²University of Pittsburgh, Pittsburgh, Pennsylvania 15260

¹³University of Puerto Rico, Mayaguez, Puerto Rico 00681

¹⁴Purdue University, West Lafayette, Indiana 47907

¹⁵Rensselaer Polytechnic Institute, Troy, New York 12180

¹⁶University of Rochester, Rochester, New York 14627

¹⁷Southern Methodist University, Dallas, Texas 75275

¹⁸Syracuse University, Syracuse, New York 13244

¹⁹Vanderbilt University, Nashville, Tennessee 37235

²⁰Wayne State University, Detroit, Michigan 48202

²¹Carleton University, Ottawa, Ontario, Canada K1S 5B6

²²Carnegie Mellon University, Pittsburgh, Pennsylvania 15213

²³Enrico Fermi Institute, University of Chicago, Chicago, Illinois 60637

(Dated: November 13, 2006)

We present measurements of the inclusive branching fractions for the decays $D^+ \rightarrow Xe^+\nu_e$ and $D^0 \rightarrow Xe^+\nu_e$, using 281 pb^{-1} of data collected on the $\psi(3770)$ resonance with the CLEO-c detector. We find $\mathcal{B}(D^0 \rightarrow Xe^+\nu_e) = (6.46 \pm 0.17 \pm 0.13)\%$ and $\mathcal{B}(D^+ \rightarrow Xe^+\nu_e) = (16.13 \pm 0.20 \pm 0.33)\%$. Using the known D meson lifetimes, we obtain the ratio $\Gamma_{D^+}^{\text{sl}}/\Gamma_{D^0}^{\text{sl}} = 0.985 \pm 0.028 \pm 0.015$, confirming isospin invariance at the level of 3%. The positron momentum spectra from D^+ and D^0 have consistent shapes.

PACS numbers: 13.20.Fc, 12.38.Qk, 14.40.Lb

The study of inclusive D semileptonic decays is important for several reasons. First, by comparing the inclusive branching fractions of the D^+ and D^0 mesons with the sum of the measured exclusive branching frac-

tions, one can determine whether there are unobserved semileptonic decay modes. Previous data suggest that the lightest vector and pseudoscalar resonances saturate the hadronic spectra [1]. This may be due to the rela-

tively low momentum of the daughter s quark, that favors the formation of s -wave hadrons. Alternatively, this may be an indication that heavy quark effective theory may still be valid at the charm quark mass scale [2]. In addition, since accurate experimental determinations of the D^0 and D^+ lifetimes are available [1], measurements of semileptonic branching fractions determine the corresponding semileptonic widths, $\Gamma_{D^+}^{\text{sl}}$ and $\Gamma_{D^0}^{\text{sl}}$. These widths are expected to be equal, modulo small corrections introduced by electromagnetic effects. Weak annihilation diagrams can produce more dramatic effects on the Cabibbo suppressed partial widths [3]. As these contributions may also influence the extraction of V_{ub} from inclusive B meson semileptonic decays, it is important to understand them well. Finally, better knowledge of the inclusive positron spectra can be used to improved modeling of the “cascade” decays $b \rightarrow c \rightarrow se^+\nu_e$ and thus is important in several measurements of b decays.

The use of ratios of semileptonic branching fractions as a probe of relative lifetimes of the D mesons was suggested by Pais and Treiman [4]. Indeed the early measurements of the ratio of the D^+ and D^0 semileptonic branching fractions gave the first surprising evidence for the lifetime difference between these two charmed mesons [5, 6]. Later, the first measurement of the individual charged and neutral D inclusive semileptonic branching fractions was performed by Mark III [7], with an overall relative error of about 12-16% on the individual branching fractions, and 19% on their ratio. The inclusive decay $D^0 \rightarrow Xe^+\nu_e$ was subsequently studied by ARGUS [8] and CLEO [9], using the angular correlation between the π^+ emitted in a $D^{*+} \rightarrow \pi^+D^0$ decay and the e^+ emitted in the subsequent $D^0 \rightarrow Xe^+\nu_e$ decay. The more precise CLEO result has a 5% relative error, dominated by systematic uncertainties. Our measurements exploit a clean $D\bar{D}$ sample at threshold, and thus achieves significantly smaller systematic errors, through low backgrounds and well understood efficiencies.

We use a 281 pb^{-1} data sample, collected at the $\psi(3770)$ center-of-mass energy ($\sqrt{s} \approx 3.73 \text{ GeV}$), with the CLEO-c detector [10]. This detector includes a tracking system composed of a six-layer low-mass drift chamber and a 47-layer central drift chamber, measuring charged particle momentum and direction, a state of the art CsI(Tl) electromagnetic calorimeter, and a Ring Imaging Cherenkov (RICH) hadron identification system. All these components are critical to an efficient and highly selective electron and positron identification algorithm. The charged particle momentum resolution is approximately 0.6% at 1 GeV. The CsI(Tl) calorimeter measures the electron and photon energies with a resolution of 2.2% at $E = 1 \text{ GeV}$ and 5% at $E=100 \text{ MeV}$, which, combined with the excellent tracking system, provides one of the e identification variables, E/p , where E is the energy measured in the calorimeter and p is the momentum measured in the tracking system. The

tracking system provides charged particle discrimination too, through the measurement of the specific ionization dE/dx . Charged particles are also identified over most of their momentum range in the RICH detector [11]. In particular, RICH identification plays a crucial role at momenta where the specific ionization bands of two particle species cross each other and dE/dx does not provide any discrimination power.

We use a tagging technique similar to the one pioneered by the Mark III collaboration [12]. Details on the tagging selection procedure are given in Ref. [13]. We select events containing either the decay $\bar{D}^0 \rightarrow K^+\pi^-$ or the decay $D^- \rightarrow K^+\pi^-\pi^-$. We use only these modes, because they have very low background. Note that charge conjugate modes are implied throughout this paper. In this analysis we exploit the flavor information provided by the tagging D : the D^- charge sign provides a flavor tag, whereas the charge of the tag daughter K is used for \bar{D}^0 flavor assignment.

We analyze all the recorded events at the $\psi(3770)$ and retain the events that contain at least one candidate $\bar{D}^0 \rightarrow K^+\pi^-$ or $D^- \rightarrow K^+\pi^-\pi^-$. Two kinematic variables are used to select these candidates: the beam-constrained mass, $M_{\text{bc}} \equiv \sqrt{E_{\text{beam}}^2 - (\Sigma_i \vec{p}_i)^2}$, and the energy difference ΔE , where $\Delta E \equiv (\Sigma_i E_i - E_{\text{beam}})$, where E_{beam} represents the beam energy and (E_i, \vec{p}_i) represent the 4-vectors of the candidate daughters. For \bar{D}^0 tags, the measured standard deviations (σ) in ΔE and M_{bc} are $\sigma(\Delta E) = 6.6 \text{ MeV}$ and $\sigma(M_{\text{bc}}) = 1.35 \text{ MeV}$, while for D^- tags, $\sigma(\Delta E) = 5.9 \text{ MeV}$ and $\sigma(M_{\text{bc}}) = 1.34 \text{ MeV}$. We select events that are within 3σ of the expected ΔE (0 GeV) and M_{bc} (M_D) for the channels considered. In order to determine the total number of tags, we count the events within the selected ΔE - M_{bc} intervals; then we subtract the combinatoric background inferred from two 3σ sideband regions on both sides of the $\Delta E = 0$ signal peak, with a 2σ gap from the signal interval. The yields in the signal region are $48204 \bar{D}^0$ and $76635 D^-$. The corresponding yields in the sideband region are 788 ± 28 and 2360 ± 49 . We correct the sideband yields with scale factors accounting for the relative area of the background in the signal and sideband intervals (1.047 for \bar{D}^0 and 1.23 for D^-). The scaling factors are inferred from the background component of the M_{bc} fits. We obtain $47379 \pm 29 \bar{D}^0$ tagged events, and $73732 \pm 60 D^-$ tagged events. As we are interested in counting the number of signal events, and not in measuring a production rate, the errors only reflect the uncertainty in the background subtraction. Note that the estimated background is only 1.7% of the signal for \bar{D}^0 and 3.9% for D^- .

For each event selected, we study all the charged tracks not used in the tagging mode. We select the ones that are well-measured, and whose helical trajectories approach the event origin within a distance of 5 mm in the projection transverse to the beam and 5 cm in the projection along the beam axis. Each track must include

at least 50% of the hits expected for its momentum. Moreover, it must be within the RICH fiducial volume ($|\cos(\theta)| \leq 0.8$), where θ is the angle with respect to the beams. Finally, we require the charged track momentum p_{track} to be greater than or equal to 0.2 GeV, as the particle species separation becomes increasingly difficult at low momenta.

Candidate positrons (and electrons) are selected on the basis of a likelihood ratio constructed from three inputs: the ratio between the energy deposited in the calorimeter and the momentum measured in the tracking system, the specific ionization dE/dx measured in the drift chamber, and RICH information [14]. Our particle identification selection criteria have an average efficiency of 0.95 in the momentum region 0.3-1.0 GeV, and 0.71 in the region 0.2-0.3 GeV.

The e^+ sample contains a small fraction of hadrons that pass our selection criteria. As the probability that a π is identified as an e at a given momentum is different from the corresponding K to e misidentification probability, we need to know the K and π yields separately to subtract this background. We select π and K samples using a particle identification variable (PID) that combines RICH and dE/dx information, if the RICH identification variable [11] is available and $p_{\text{track}} > 0.7$ GeV; alternatively PID relies on dE/dx only. The π sample contains also a μ component, as our PID variable is not very selective; however, as our goal is only to unfold the true e spectrum, we do not need to correct for this effect.

We separate e , π , and K into “right-sign” and “wrong-sign” samples according to their charge correlation to the flavor tag. Right-sign assignment is based on the expected e charge on the basis of the flavor of the decaying D . The true e populations in the right-sign and wrong-sign samples are obtained through an unfolding procedure, using the matrix:

$$\begin{pmatrix} n_e^m \\ n_\pi^m \\ n_K^m \end{pmatrix} = \begin{pmatrix} \varepsilon_e & f_{e\pi} & f_{eK} \\ f_{\pi e} & \varepsilon_\pi & f_{\pi K} \\ f_{Ke} & f_{K\pi} & \varepsilon_K \end{pmatrix} \times \begin{pmatrix} n_e^t \\ n_\pi^t + \kappa n_\mu^t \\ n_K^t \end{pmatrix};$$

here n_e^m , n_π^m , n_K^m represent the raw measured spectra in the corresponding particle species, and the coefficient κ accounts for the fact that the efficiencies for π and μ selection are not necessarily identical, especially at low momenta. The quantities n_e^t , n_π^t , and n_K^t represent the true e , π and K spectra: the present paper focuses on the extraction of n_e^t . As the π to e misidentification probability is quite small, the effect of a small μ component in the measured π population n_π^m is negligible. The efficiencies ε_e , ε_π , and ε_K account for track finding, track selection criteria, and particle identification losses. The tracking efficiencies are obtained from a Monte Carlo simulation of $D\bar{D}$ events in the CLEO-c detector. The generator incorporates all the known D decay properties, includes initial state radiation (ISR), and final state radiation (FSR)

effects, the latter are modeled with the program PHOTOS [15]. The particle identification efficiencies are determined from data. We study the K selection efficiencies using a sample of $D^+ \rightarrow K^-\pi^+\pi^+$ decays, and π selection efficiencies using $D^+ \rightarrow K^-\pi^+\pi^+$ and $K_S^0 \rightarrow \pi^+\pi^-$ decays. The e^+ identification efficiency is extracted from a radiative Bhabha sample. A correction for the difference between the $D\bar{D}$ event environment and the simpler radiative Bhabha environment (two charged tracks and one shower) is derived using a Monte Carlo sample where a real electron track stripped from a radiative Bhabha event is merged with tracks from a simulated hadronic environment. The off-diagonal elements are products of tracking efficiencies and particle misidentification probabilities, where f_{ab} is defined as the probability that particle b is identified as particle a . The f_{ab} parameters are determined using e samples from radiative Bhabhas, and K and π from $D^+ \rightarrow K^-\pi^+\pi^+$ and $K_S^0 \rightarrow \pi^+\pi^-$. The e spectrum from radiative Bhabhas is divided in 50 MeV momentum bins to determine the corresponding misidentification probabilities, whereas the K and π populations are subdivided into 100 MeV momentum bins to reduce the statistical uncertainty. The hadron to e^+ misidentification probabilities are of the order of 0.1% over most of the momentum range and below 1% even in the regions where dE/dx separation is less effective.

There are background sources that are charge symmetric, mostly produced by π^0 Dalitz decays and γ conversions. We subtract the wrong sign unfolded yields from the corresponding right sign yields to account for them, motivated by Monte Carlo studies that confirm the accuracy of this method.

In order to subtract the combinatoric background, we repeat the unfolding procedure determining the true e^+ yields from measured e^+ , π^+ , and K^+ samples where the tags are selected from ΔE sidebands. The decays $\bar{D}^0 \rightarrow K^+\pi^-$ and $D^- \rightarrow K^+\pi^-\pi^-$ have very little background: the \bar{D}^0 sidebands give a combinatoric background estimate that is 0.2% of the signal yield and the D^- sidebands give a combinatoric background estimate that is 1.8% of the signal yield. Table I shows the results of the intermediate steps involved in the determination of the net e^+ yields. Efficiency corrections increase unfolded e^+ yields with respect to uncorrected e^+ yields, while the subtraction of the contribution from misidentified hadrons reduces them. The former effect is dominant for the right-sign positron sample, while it is comparable in size to the background subtraction in the wrong-sign sample. The final yields, identified as “corrected net e^+ ” include acceptance corrections related to the $(\cos \theta \leq 0.8)$ cut, and doubly-Cabibbo suppressed (DCSD) effects in D^0 decays. As we are using the charge of the tagging D^- , rather than its K daughter charge, this correction is not needed in the charged mode.

In order to extract the partial branching fractions for $p_e \geq 0.2$ GeV, we evaluate the ratio between the net

TABLE I: Positron unfolding procedure and corrections. The errors reported in the intermediate yields reflect only statistical uncertainties.

| | D^+ | D^0 |
|-----------------------|-----------------|---------------|
| Signal e^+ | | |
| Right-sign | 8275 ± 91 | 2239 ± 47 |
| Wrong-sign | 228 ± 15 | 233 ± 15 |
| Right-sign (unfolded) | 9186 ± 103 | 2453 ± 54 |
| Wrong-sign (unfolded) | 231 ± 19 | 203 ± 19 |
| Sideband e^+ (RS) | 168 ± 13 | 15 ± 4 |
| Sideband e^+ (WS) | 11 ± 5 | 11 ± 4 |
| Net e^+ | 8798 ± 105 | 2246 ± 57 |
| Corrected Net e^+ | 10998 ± 132 | 2827 ± 72 |

positron yields corrected for geometric acceptance and the net number of tags. While the charge of $D^- \rightarrow K^+\pi^-\pi^-$ reliably tags the flavor of the charged D , in the \bar{D}^0 case the K charge occasionally produces an incorrect flavor assignment due to the DCSD $\bar{D}^0 \rightarrow K^-\pi^+$. This effect is estimated on the basis of the known value of the parameter $r_{\text{DCSD}} \equiv N(D^0 \rightarrow K^+\pi^-)/N(D^0 \rightarrow K^-\pi^+) = 0.00362 \pm 0.00029$ [1].

We have considered several sources of systematic uncertainties. There are multiplicative errors that affect the overall scale of the spectrum, including tracking efficiency or electron identification efficiency, accounting for Monte Carlo modeling uncertainties. The uncertainties in tracking and K and π identification efficiencies are taken from the studies discussed in Ref. [13]. The systematic error on the electron identification efficiency (1%) is assessed by comparing radiative Bhabha samples, radiative Bhabha tracks embedded in $D\bar{D}$ Monte Carlo samples, and $D\bar{D}$ Monte Carlo samples. These contributions are common to D^+ and D^0 . In addition, we have accounted for the FSR uncertainty by varying its amount, with a total systematic error of 0.5%. The last multiplicative error is the uncertainty on the number of tags, estimated by comparing the number of background tags in our signal window from the ΔE sidebands and from M_{bc} sidebands. In addition, there are terms that are affected by limited statistics, such as misidentification probabilities, or particle identification efficiencies. The systematic uncertainty associated with these terms is evaluated with a toy Monte Carlo; we perform 10^6 iterations of the unfolding procedure, and vary the matrix elements within error. The corresponding relative systematic error estimates are 0.56% (statistical errors on particle misidentification probability and particle identification efficiency) and 0.3% (statistical error on tracking efficiency). The uncertainty on the combinatoric background, accounted for with the sideband positron sample, is negligible compared with these components ($\leq 0.1\%$), because of the excellent purity of the tag samples used. Thus the total relative systematic error on the branching

fraction for $p_e \geq 0.2$ GeV is 1.7% (D^0) and 1.8 % (D^+).

The partial branching fractions for $p_e \geq 0.2$ GeV are evaluated as the ratio between the corrected net e yields and the net number of tags:

$$\mathcal{B}(D^+ \rightarrow Xe^+\nu_e) = (14.92 \pm 0.19_{\text{stat}} \pm 0.27_{\text{sys}})\%;$$

$$\mathcal{B}(D^0 \rightarrow Xe^+\nu_e) = (5.97 \pm 0.15_{\text{stat}} \pm 0.10_{\text{sys}})\%.$$

The yield in the unmeasured region ($p_e < 0.2$ GeV) is estimated by fitting the measured spectra with a shape derived from Monte Carlo. The semileptonic decays are generated with the ISGW form factor model [16], with parameters tuned to experimental constraints such as measured branching fractions, with the procedure described in Ref. [9]. Final state radiation effects are included in the simulation. We obtain $f(p_e) \equiv \Delta\Gamma_{\text{sl}}(p_e < 0.2 \text{ GeV})/\Gamma_{\text{sl}} = (7.5 \pm 0.5)\%$ for $D^+ \rightarrow Xe^+\nu_e$ and $\Delta\Gamma_{\text{sl}}(p_e < 0.2 \text{ GeV})/\Gamma_{\text{sl}} = (7.7 \pm 0.9)\%$ for $D^0 \rightarrow Xe^+\nu_e$. The χ^2 per degree of freedom is 1.23 for $D^+ \rightarrow Xe^+\nu_e$, 0.75 for $D^0 \rightarrow Xe^+\nu_e$. We studied the sensitivity of our analysis to $f(p_e)$ using alternative fitting procedures, such as a combination of the dominant exclusive channels modeled with different form factors [2]. The fractional difference in $f(p_e)$ with the various methods considered is below 4% and is well within the systematic errors assigned. Note that the relative error in the branching fraction introduced by the extrapolation to the unmeasured portion of the spectrum is given $\delta f(p_e)/(1 - f(p_e))$, and thus the systematic error on the total semileptonic branching fractions is a about 1%. Upon applying this correction, we obtain:

$$\mathcal{B}(D^+ \rightarrow Xe^+\nu_e) = (16.13 \pm 0.20_{\text{stat}} \pm 0.33_{\text{sys}})\%;$$

$$\mathcal{B}(D^0 \rightarrow Xe^+\nu_e) = (6.46 \pm 0.17_{\text{stat}} \pm 0.13_{\text{sys}})\%.$$

Using the well-measured lifetimes of the D^+ and D^0 mesons, $\tau_{D^+} = (1.040 \pm 0.007)$ ps, and $\tau_{D^0} = (0.4103 \pm 0.0015)$ ps [1], we normalize the measured partial branching fractions to obtain differential semileptonic widths $d\Gamma^{\text{sl}}/dp_e$ in the laboratory frame, where the D^+ momentum is 0.243 GeV, and the D^0 momentum is 0.277 GeV. No final state radiation correction is applied to the data points. Table II shows the corresponding numerical values. The errors shown are evaluated by adding the statistical errors and the additive systematic errors in quadrature. In addition, an overall multiplicative systematic error of about 1.5% needs to be included in derived quantities such as the total semileptonic width to account for overall tracking and particle identification efficiency uncertainties. The total inclusive semileptonic widths are $\Gamma(D^+ \rightarrow Xe^+\nu_e) = 0.1551 \pm 0.0020 \pm 0.0031 \text{ ps}^{-1}$, and $\Gamma(D^0 \rightarrow Xe^+\nu_e) = 0.1574 \pm 0.0041 \pm 0.0032 \text{ ps}^{-1}$. The corresponding ratio of the semileptonic widths

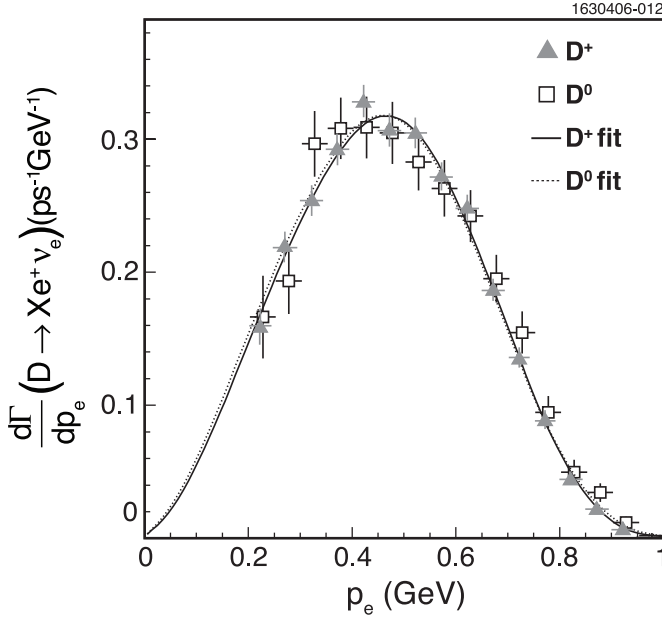


FIG. 1: Positron differential semileptonic widths $d\Gamma^{\text{sl}}/dp_e$ for the decays $D^0 \rightarrow Xe^+\nu_e$ (open squares) and $D^+ \rightarrow Xe^+\nu_e$ (filled triangles) in the laboratory frame. The errors shown include statistical and additive systematic errors. The symbols for D^+ and D^0 spectra are slightly shifted horizontally to avoid overlapping. The curves are derived from the fits used to extrapolate the measured spectra below the p^{min} cut.

TABLE II: D^+ and D^0 positron differential semileptonic widths $d\Gamma/dp_e$ ($\text{ps}^{-1}\text{GeV}^{-1}$) in the laboratory frame. The errors shown include statistical errors and additive systematic errors.

| p_e (GeV) | $d\Gamma/dp_e(D^+)$ | $d\Gamma/dp_e(D^0)$ |
|-------------|---------------------|---------------------|
| 0.20 - 0.25 | 0.1598 ± 0.0142 | 0.1664 ± 0.0311 |
| 0.25 - 0.30 | 0.2185 ± 0.0121 | 0.1935 ± 0.0248 |
| 0.30 - 0.35 | 0.2538 ± 0.0116 | 0.2966 ± 0.0247 |
| 0.35 - 0.40 | 0.2925 ± 0.0121 | 0.3081 ± 0.0231 |
| 0.40 - 0.45 | 0.3281 ± 0.0127 | 0.3088 ± 0.0233 |
| 0.45 - 0.50 | 0.3064 ± 0.0130 | 0.3047 ± 0.0233 |
| 0.50 - 0.55 | 0.3047 ± 0.0115 | 0.2828 ± 0.0214 |
| 0.55 - 0.60 | 0.2716 ± 0.0111 | 0.2631 ± 0.0212 |
| 0.60 - 0.65 | 0.2479 ± 0.0104 | 0.2422 ± 0.0196 |
| 0.65 - 0.70 | 0.1864 ± 0.0088 | 0.1951 ± 0.0179 |
| 0.70 - 0.75 | 0.1359 ± 0.0076 | 0.1547 ± 0.0158 |
| 0.75 - 0.80 | 0.0892 ± 0.0060 | 0.0948 ± 0.0121 |
| 0.80 - 0.85 | 0.0444 ± 0.0042 | 0.0498 ± 0.0091 |
| 0.85 - 0.90 | 0.0221 ± 0.0028 | 0.0344 ± 0.0070 |
| 0.90 - 0.95 | 0.0065 ± 0.0015 | 0.0120 ± 0.0044 |
| 0.95 - 1.00 | 0.0007 ± 0.0005 | 0.0020 ± 0.0020 |

of charged and neutral D mesons is $\Gamma_{D^+}^{\text{sl}}/\Gamma_{D^0}^{\text{sl}} = 0.985 \pm 0.028 \pm 0.015$, consistent with isospin invariance.

Finally, we can compare these widths with the sum of the semileptonic decay widths for the pseudoscalar and vector hadronic final states recently published by CLEO [17]: $\mathcal{B}(D^+ \rightarrow Xe^+\nu_e)_{\text{excl}} = (15.1 \pm 0.5 \pm 0.5)\%$ and

$\mathcal{B}(D^0 \rightarrow Xe^+\nu_e)_{\text{excl}} = (6.1 \pm 0.2 \pm 0.2)\%$: the measured exclusive modes are consistent with saturating the inclusive widths, although there is some room left for higher multiplicity modes. The composition of the inclusive hadronic spectra is dominated by the low lying resonances in the $c \rightarrow s$ and $c \rightarrow d$, in striking contrast with B semileptonic decays, where a sizeable component of the inclusive branching fraction is still unaccounted for [1].

In conclusion, we report improved measurements of the absolute branching fractions for the inclusive semileptonic decays $\mathcal{B}(D^+ \rightarrow Xe^+\nu_e) = (16.13 \pm 0.20 \pm 0.33)\%$ and $\mathcal{B}(D^0 \rightarrow Xe^+\nu_e) = (6.46 \pm 0.17 \pm 0.13)\%$. Using the measured D meson lifetimes, the ratio $\Gamma_{D^+}^{\text{sl}}/\Gamma_{D^0}^{\text{sl}} = 0.985 \pm 0.028 \pm 0.015$ is extracted, and it is consistent with isospin invariance. The shapes of the spectra are consistent with one another within error.

ACKNOWLEDGEMENTS

We gratefully acknowledge the effort of the CESR staff in providing us with excellent luminosity and running conditions. This work was supported by the A.P. Sloan Foundation, the National Science Foundation, the U.S. Department of Energy, and the Natural Sciences and Engineering Research Council of Canada.

* Current address: Universität Bonn, Nussallee 12, D-53115 Bonn

- [1] S. Eidelman *et al.*, Phys. Lett. B **592**, 1 (2004).
- [2] D. Scora and N. Isgur, Phys. Rev. D **52**, 2783 (1995) [arXiv:hep-ph/9503486].
- [3] S. Bianco, F. L. Fabbri, D. Benson and I. Bigi, Riv. Nuovo Cim. **26N7**, 1 (2003) [arXiv:hep-ex/0309021].
- [4] A. Pais and S. B. Treiman, Phys. Rev. D **15**, 2529 (1977).
- [5] R. H. Schindler *et al.* [Mark II Collaboration], Phys. Rev. D **24**, 78 (1981).
- [6] W. Bacino *et al.* [DELCO Collaboration], Phys. Rev. Lett. **45**, 329 (1980).
- [7] R. M. Baltrusaitis *et al.* [Mark III Collaboration], Phys. Rev. Lett. **54**, 1976 (1985) [Erratum-ibid. **55**, 638 (1985)].
- [8] H. Albrecht *et al.* [ARGUS Collaboration], Phys. Lett. B **374**, 249 (1996).
- [9] Y. Kubota *et al.* [CLEO Collaboration], D **54**, 2994 (1996).
- [10] Y. Kubota *et al.*, Nucl. Instrum. Meth. A **320**, 66 (1992).
- [11] M. Artuso *et al.*, Nucl. Instrum. Meth. A **502**, 91 (2003) [arXiv:hep-ex/0209009].
- [12] J. Adler *et al.* [Mark III Collaboration], Phys. Rev. Lett. **62**, 1821 (1989).
- [13] Q. He *et al.* [CLEO Collaboration], Phys. Rev. Lett. **95**, 121801 (2005) [arXiv:hep-ex/0504003].
- [14] T. E. Coan *et al.* [CLEO Collaboration], Phys. Rev. Lett. **95**, 181802 (2005) [arXiv:hep-ex/0506052].

- [15] E. Barberio and Z. Was, Comput. Phys. Commun. **79**, 291(1994).
- [16] N. Isgur, D. Scora, B. Grinstein and M. B. Wise, Phys. Rev. D **39**, 799 (1989).
- [17] G. S. Huang *et al.* [CLEO Collaboration], Phys. Rev. Lett. **95**, 181801 (2005) [arXiv:hep-ex/0506053].